International Research Journal on Advanced Engineering Hub (IRJAEH)
e ISSN: 2584-2137
Vol. 03 Issue: 01 January 2025
Page No: 52-60
https://irjaeh.com
https://doi.org/10.47392/IRJAEH.2025.0007

Transfer Learning-Based Convolutional Neural Network for Six - Class Lung Disease Classification

M.V.S. Sairam[1], Raju Egala[2]
[1]Professor, Department of ECE, Gayatri Vidya Parishad College of Engineering (A), Visakhapatnam, AP, India.
[2]Assistant Professor, Department of ECE, Gayatri Vidya Parishad College for Degree and PG Courses (A), Visakhapatnam, AP, India.
Emails: *sairammvs3@gmail.com[1], 402.raju@gmail.com[2]*

Abstract
Convolutional neural network (CNN)-based deep learning (DL) is a promising solution in several applications, such as image classification and computer vision. Further, transfer learning-based CNN (TL-CNN) supports objective-specific applications, which can be achieved by integrating a pre-trained model such as Visual Geometry Group19 (VGG19) with a customized network. In the present work, convolution layers, ReLU functions, and pooling layers in the customized network are strategically chosen to classify six-class lung diseases: pneumonia, cardiomegaly, lung opacity, tuberculosis (TB), COVID-19, and normal. Also, the hyper parameters are optimized to refine the extended-VGG19 architecture (VGG19+customized network) in TL-CNN. The TL-CNN was built using Kaggle dataset of 3802 chest X-ray (CXR) images. Testing was conducted to evaluate the created TL-CNN, and the findings confirm that the proposed work outperformed existing models with 93.85% accuracy, 94.04% precision, 93.85% recall, 93.82% F1 score, and 99.56% area under the curve (AUC). Moreover, the confusion matrix of the TL-CNN is also discussed to access the distinguishability of the proposed multiclass classification.

Keywords: *DL, CNN, Transfer learning, accuracy, AUC, confusion matrix*

1. Introduction
Nowadays, the integration of medicine and artificial intelligence (AI) has experienced significant enhancement in medical imaging analysis. The field of AI could mimic human intelligence. The ML subset of AI shifted focus from rule-based systems to algorithms that could learn from data. The ML algorithms depend on manual feature extraction, requiring human intervention. DL, a subset of ML, fetched the capabilities of AI, using neural networks with multiple layers, enabling the system to automatically extract features [1-3]. This is beneficial in medical imaging analysis, where manually extracting features from a large dataset can be challenging. CXR images are mostly preferred modalities for lung diseases due to their detailed imaging analysis. After the COVID-19 pandemic, respiratory systems are being attacked by a variety of lung diseases that can trigger similar symptoms. Many authors presented DL algorithms for classifying lung diseases [2-5], [8], [10-24].

1.1 Convolutional Neural Networks
CNN is one of the prevalent architectures in DL, consisting of convolutional layers, activation layers, pooling layers, and fully connected layers [6-9]. Convolutional layers are responsible for feature extraction. Grouped convolution can also be employed, leading to efficient utilization of the Graphics Processing Unit (GPU) system. Activation functions introduce non-linearity to model complex patterns in the images. The widely used activation layers in CNNs are Rectified Linear Unit (ReLU) and Sigmoid. Pooling layers downsample the dimensions of feature maps, reducing the computational load, and introducing spatial invariance. The commonly used pooling methods are max pooling, sum pooling, and average pooling. Then after, features learned by the network are flattened and passed into fully connected layers. The final fully connected layer uses an activation function like softmax, converting output into probabilities, representing the likelihood of each class. In CNN, learning rate (l_r), number of epochs

International Research Journal on Advanced Engineering Hub (IRJAEH)
e ISSN: 2584-2137
Vol. 03 Issue: 01 January 2025
Page No: 52-60
https://irjaeh.com
https://doi.org/10.47392/IRJAEH.2025.0007

(e_n), and batch size (b_s) are critical hyper parameters [2, 4]. These parameters are to be carefully optimized to maximize the performance. The models like VGG16 and VGG19, which are pre-trained on huge datasets such as ImageNet, are decisive for research without the need to design from scratch, saving time and computational resources. Also, frameworks like TensorFlow and PyTorch can access these models simply. These pre-trained models have been used by developers to solve real world problems. Various pre-trained models are listed in Table 1.

Table 1 Pre-Trained CNN Models

Model	Year	Applications
LeNet	1998	Handwritten digit recognition
AlexNet	2012	Image classification, computer vision
VGG16	2014	Image classification
VGG19	2014	Deeper version of VGG16
GoogLeNet (Inception)	2014	Image classification, object detection
ResNet	2015	Image classification, object detection
DenseNet	2016	Image classification
Xception	2016	Image classification, object detection
MobileNet	2017	Image recognition for mobile and embedded devices
BERT	2018	Natural language processing
EfficientNet	2019	Image classification, object detection
Vision Transformer	2020	Image classification, transfer learning
Swin Transformer	2021	Image classification, object detection
ConvNeXt	2022	Image classification, object detection

In the present work, VGG19 was used as the core CNN which was developed by researchers at the University of Oxford.

1.2 Transform Learning

Transfer learning is used in deep learning to customize an already available pre-trained model to a specific task. As depicted in Figure 1, the extended-pre-trained model consists of a pre-trained model, integrated with an additional customized network.

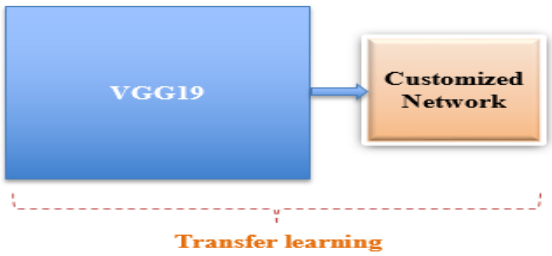

Figure 1 Extended-Pre-Trained Model

The pre-trained model, having been trained on a general dataset, learned useful features like edges and textures of the images. The layers in the customized network are trained on an objective-specific dataset to support distinct applications [1]. The remaining part of the work is organized as follows: Section 2 outlines the literature review related to the work. The proposed transfer learning-based CNN is described in Section 3. Section 4 incorporates the experimental framework. Section 5 discusses the results, and comparative analysis is provided in Section 6. Finally, the conclusion and future scope are presented.

2. Literature Review

The focus of this section is to explore CNN-based DL models presented by many authors for the classification of lung diseases I. Sirazitdinov et al.[8] proposed RetinaNet and Mask R-CNN models to classify lung opacity, lung cancer, and normal cases from CXR images, attaining an accuracy of 83% with a precision of 75% and recall of 79%. Lower performance metrics indicate scope for further improvement. Integrating AlexNet, GoogleNet, and ResNet by R. Hooda et al. [12] for binary classification of TB and non-TB cases from CXR images achieved an accuracy of 88.24%, precision and recall of 88% and 88.42%, respectively. In 2020, J. Zhang et al.[19], recommended a CNN binary classifier for COVID-19 and normal with CXR images. The model achieved an accuracy of 72.77%, precision of 73.83%, and sensitivity of 71.7%. Even so, there's a possibility of overfitting, i.e., the model is ineffective on unseen data N. Tsiknakis et al. [20] presented an Inception-v3 to classify pneumonia,

International Research Journal on Advanced Engineering Hub (IRJAEH)
e ISSN: 2584-2137
Vol. 03 Issue: 01 January 2025
Page No: 52-60
https://irjaeh.com
https://doi.org/10.47392/IRJAEH.2025.0007

COVID-19, and normal cases. The model achieved an accuracy of 76%, precision of 87%, and sensitivity of 93%. However, the complexity of Inception-v3 needs more computational resources. The absence of an F1 score also limits a complete assessment of the model. ResNet32 with transfer learning presented by Y. Pathak et al. [16] in 2020 for classifying COVID-19 cases from computed tomography (CT) images attained an accuracy of 93%, with precision of 95% and recall of 91%. This work can be extended by using the recent dataset. Bai HX et al. [5] used reverse transcription polymerase chain reaction (RTPCR) data along with CXR images to differentiate pneumonia and COVID-19, achieving an accuracy of 83% with high precision (94%), and recall (93%). Lower accuracy and dependency on RTPCR data constrain reliability. Varalakshmi Perumal et al. [2] combined VGG16, ResNet50, and InceptionV3 to classify CXR and CT images, achieving an accuracy of 93%, precision and recall of 91% and 90%, respectively. The multi-model approach is complex to implement. Debabrata Dansana et al. [18] used VGG-16, InceptionV2, and decision tree models to classify COVID-19 from CXR images and CT images, achieving an accuracy of 91% with precision of 94% and recall of 97%. There is a scope for enhancing accuracy further.

A binary classifier was developed in 2020 by Oh Y et al. [21], using CNN for COVID-19 and normal from CXR images, achieving an accuracy of 88.9%, precision and recall of 83.4% and 85.9%, respectively. Shayan Hassantabar et al. [22] used both CXR and CT images with CNN to classify COVID-19 and normal, achieving an accuracy of 93.2%, precision (78%), and recall (86%). Lower precision leads to a higher rate of false positive. An accuracy of 81.4%, precision and recall of 79.8% and 87.5%, respectively, was achieved from the binary model for COVID-19 developed by C. Li, D. et al. [15] in 2020 via. D-Resnet-10 from CT images. X.W. Gao, C. et al. [11] recommended Depth-ResNet to classify TB and non-TB cases from CT images, achieving an accuracy of 85.29% with precision of 84%, and recall of 84.16%. C. Sitaula et al. [17] proposed VGG16 to classify COVID-19, bacterial pneumonia, viral pneumonia, and normal from CXR images, achieving an accuracy of 79% with precision and recall of 92% and 95%, respectively. Lower performance suggests the need for further improvement. Y. Song et al. [4] developed the DRE-Net model to classify pneumonia, COVID-19, and normal cases from CT images, achieving an accuracy of 86% with precision of 96% and recall of 93%. Lower accuracy leads to misclassification. In 2023, Minalu Chalie et al. [14] integrated VGG16, VGG19, ResNet50V2, and DenseNet201 models to classify TB, pneumonia, pleural effusion, normal from CXR images, achieving an accuracy of 92%, precision and recall of 91% and 89%, respectively. There is scope for enhancing the performance. The comprehensive survey provides valuable insights in medical image analysis to carry out the present work.

3. Proposed Transfer Learning-Based Cnn Model

The proposed TL-CNN for six-class lung diseases classification is shown in Figure 2.

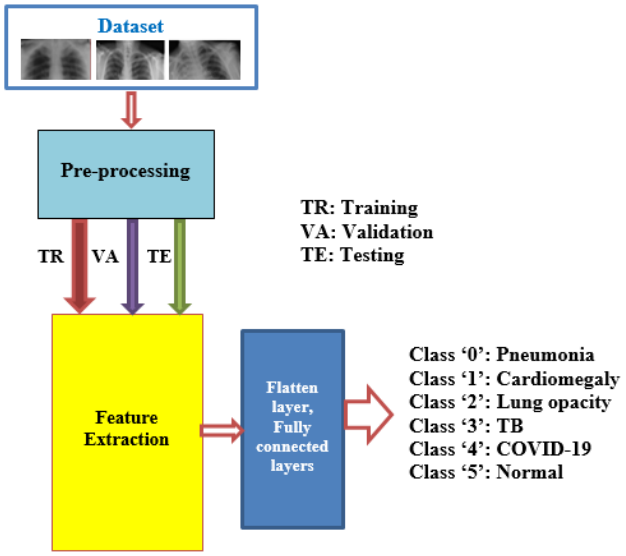

Figure 2 Proposed Transfer Learning-Based CNN

The images are resized to a uniform dimension of 224x224x3 pixels with color channels (red, green, blue) and normalized pixel values in the range [0, 1] during the pre-processing stage. Then, pre-processing, the dataset is separated into three sets: training, validation, and testing. The model is trained using the Adam optimizer [25]. The extended-VGG19 architecture that extracted features using the

International Research Journal on Advanced Engineering Hub (IRJAEH)
e ISSN: 2584-2137
Vol. 03 Issue: 01 January 2025
Page No: 52-60
https://irjaeh.com
https://doi.org/10.47392/IRJAEH.2025.0007

transfer learning technique is depicted in Figure 3.

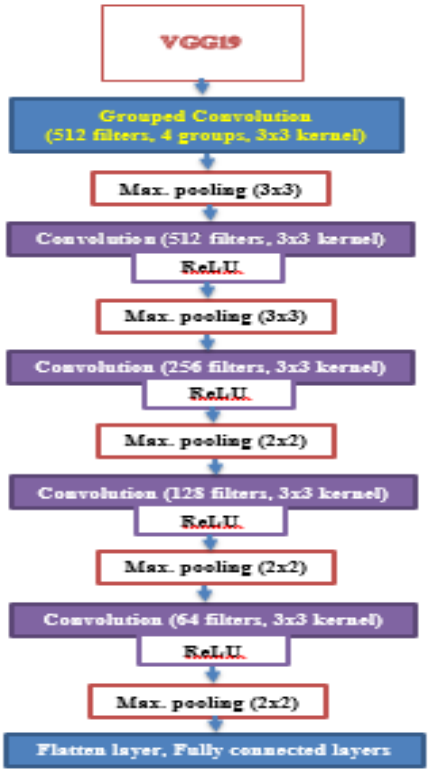

Figure 3 Extended-VGG19 Architecture

The transfer learning is performed by integrating VGG19 with a customized network, wherein layers were strategically customized to accomplish the objective of the present work. Initially, a layer with grouped convolution (512 filters) was divided into four groups with a 3x3 kernel. The architecture then follows a cascade of convolutional layers with decreasing filter sizes (512, 256, 128, and 64), each using 3x3 kernels and ReLU activation functions. Max pooling layers are interspersed with varying pool sizes (3x3 and 2x2), letting the network progressively reduce spatial dimensions and capture hierarchical features. The final layers consist of flattening and passing the extracted feature into fully connected layers. The fully connected layers classify the images according to the learned features. The customized feature extraction architecture was employed in the CNN to classify multiple lung diseases, and the performance is discussed in the subsequent section. The steps involved in the present work are summarized below. Table 2 shows Dataset.

Table 2 Dataset

I	:	Input		Dataset: 3802 images of Pneumonia, Cardiomegaly, Lung opacity, TB, COVID-19, Normal
II	:	Preprocessing		Resize Images to 224x224x3 Normalize images pixel values in the interval [0,1]
III	:	Divide dataset		Training (70%), Validation (15%) Testing (15%)
IV	:	Training & Validation		Extended-VGG19
V	:	Testing		Classification: Class: 0/1/2/3/4/5

4. Experimental Framework

The proposed model was created using an open-source programming language, Python 3. It includes several libraries like Keras for model construction, TensorFlow for backend operations, NumPy and Pandas for data pre-processing, and Scikit-learn for deriving the evaluation matrices. The model presented in the preceding section was executed on a licensed service, the Google Colab Pro platform, which provides advanced computational capabilities. Specifically, the Colab Pro environment includes 2 TB of storage, 25 GB of RAM, and access to an NVIDIA P100 GPU [25]. The dataset of 3802 images with six classes (0 through 5) was collected from the publicly available platform Kaggle [26]. The dataset was divided as shown in Figure 4.

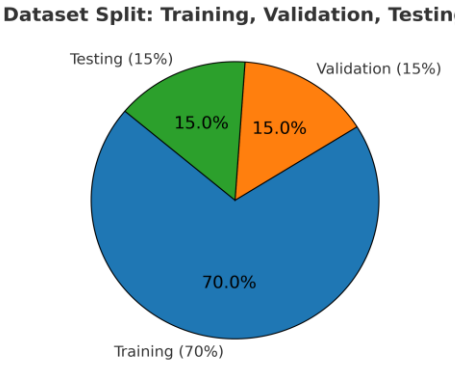

Figure 4 Dataset: Training, Validation and Testing

International Research Journal on Advanced Engineering Hub (IRJAEH)
e ISSN: 2584-2137
Vol. 03 Issue: 01 January 2025
Page No: 52-60
https://irjaeh.com
https://doi.org/10.47392/IRJAEH.2025.0007

5. Results and Discussion

The training was conducted in the fully connected layers with hyperparameters: l_r, e_n, and b_s found to be 10^{-5}, 20, and 32, respectively. Figure 5 Training And Validation Performance of Accuracy, and performance is summarized in Tables (a):(b), respectively. Figure 6 Training and Validation Performance Loss.

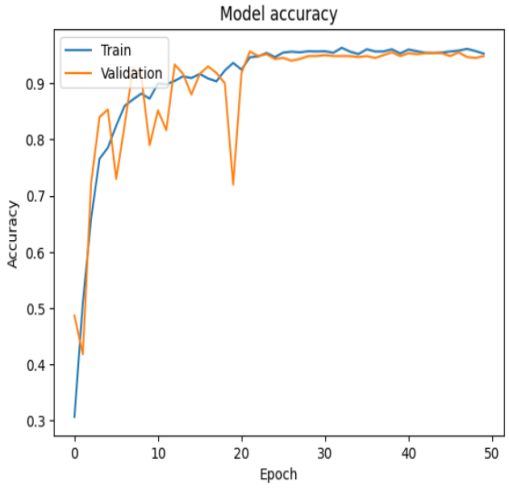

Figure 5 Training And Validation Performance of Accuracy

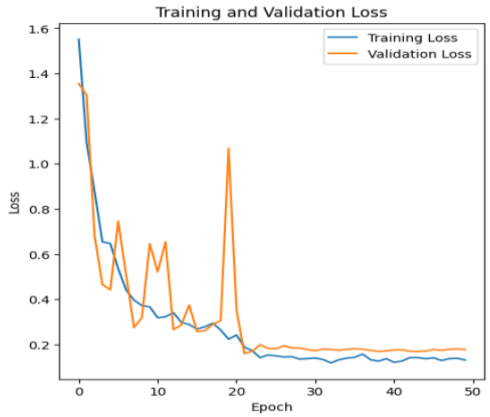

Figure 6 Training and Validation Performance Loss

From Figures and Tables, it can be noted that both training and validation accuracy increase significantly in the early epochs. Around the 20th epoch, the training accuracy stabilizes between 0.95 and 0.98, while the validation accuracy fluctuates but remains 0.90 to 0.93. From Figure 5(b) and Table 2(b), it is seen that both training and validation loss decrease abruptly during the first 10 epochs, confirming the model is quickly minimizing errors. However, fluctuations during epochs 10 to 20 in validation loss indicates that the model is temporarily overfitting to the training data. Both training and validation loss stabilize after 20 epochs and display a balanced state. AUC for the present work is depicted in Figure 6. The AUC values for classes '0', '1', '2', and '3' are 1, indicating that the model distinguishes these classes perfectly. Classes '4' and '5', the values are 0.99, denote a small error in classification. Table 3 shows Accuracy of Training and Validation Table 4 shows Loss of Training and Validation.

Table 3 Accuracy of Training and Validation

n_e	Accuracy	
	Training	Validation
1	0.35	0.3
5	0.78	0.74
10	0.85	0.83
15	0.9	0.86
20	0.94	0.89
25	0.96	0.91
30	0.96	0.91
35	0.97	0.92
40	0.98	0.93
45	0.98	0.93
50	0.98	0.93

Table 4 Loss of Training and Validation

n_e	Loss	
	Training	Validation
1	1.5	1.4
5	0.5	0.6
10	0.26	0.42
15	0.2	0.32
20	0.15	0.27
25	0.12	0.22
30	0.11	0.2
35	0.1	0.17
40	0.09	0.16
45	0.09	0.15
50	0.09	0.15

International Research Journal on Advanced Engineering Hub (IRJAEH)
e ISSN: 2584-2137
Vol. 03 Issue: 01 January 2025
Page No: 52-60
https://irjaeh.com
https://doi.org/10.47392/IRJAEH.2025.0007

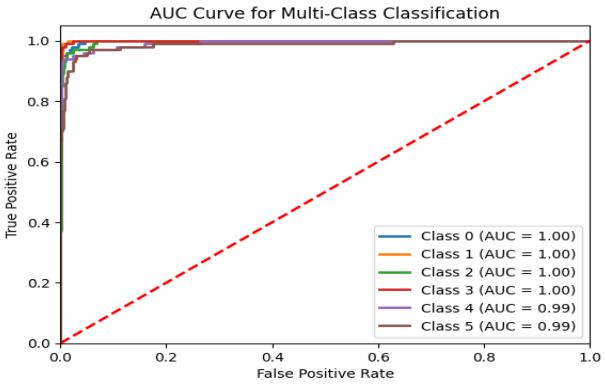

Figure 6 Area under the Curve

The model achieved an AUC of 99.56%, i.e., it correctly classifies the CXR images in 99.56% of cases. This remarkable performance confirms the discriminatory ability of the present work. The created model was evaluated on test data, and the performance is summarized in Table 3. Additionally, a confusion matrix for the test data of the present work is provided to access the distinguishability of the TL-CNN in Figure 7. Table 3 shows Performance of the TL-CNN Model

Table 3 Performance of the TL-CNN Model

Accuracy	Precision	Recall	F1 score	AUC
93.85%	94.04%	93.85%	93.82%	99.56%

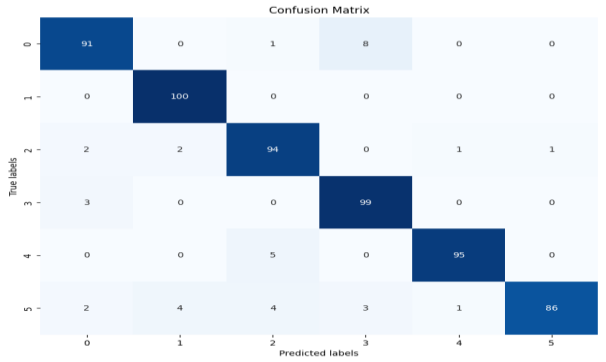

Figure 7 Confusion Matrix for the Proposed Model

The rows and columns represent the actual and prediction classes. The diagonal cells represent perfect classifications, while off-diagonal cells represent misclassifications. Out of 602 images in test data, the confusion matrix confirms that class '0' has 91 correctly classified images, with 1 image being misclassified as class '2' and 8 images being misclassified as class '3'. Similarly, class '1' has perfect classification with all 100 images. The performance metrics can also be derived from Equations (1-4) [27].

$$Accuracy = \frac{TP + TN}{TP + TN + FP + FN} \quad (1)$$

$$Precision = \frac{TP}{TP + FP} \quad (2)$$

$$Recall = \frac{TP}{TP + FN} \quad (3)$$

$$F1\ Score = \frac{2TP}{2TP + FP + FN} \quad (4)$$

TP = actual positive; TN = actual negative
FP = false positive; FN = false negative

The proposed TL-CNN model's Python code was published on the publicly available websites Kaggle [29] and GitHub [30].

6. Comparative Analyses

The performance of the TL-CNN is compared with models developed by many authors in Table 4, and the performance can be clearly visualized in Figures 8(a) :(e). Table 4 shows Comparative Analysis.

Table 4 Comparative Analysis

Ref.	N	A	P	R	F
[4]	3	86%	96%	93%	-
[8]	2	83%	75%	79%	83%
[11]	2	85.29%	54%	81.16%	-
[12]	2	88.24%	88%	88.42%	88%
[14]	4	92%	91%	89%	-
[15]	2	81.4%	79.8%	87.5%	-
[16]	2	93%	95%	91%	-
[17]	5	79%	92%	95%	-
[18]	2	91%	94%	97%	-
[19]	2	72.77%	73.83%	71.7%	-
[20]	3	76%	87%	93%	-
[21]	2	88.9%	83.4%	85.9%	96.4%
Pro	**6**	**93.85%**	**94.04%**	**93.85%**	**93.82%**

International Research Journal on Advanced Engineering Hub (IRJAEH)
e ISSN: 2584-2137
Vol. 03 Issue: 01 January 2025
Page No: 52-60
https://irjaeh.com
https://doi.org/10.47392/IRJAEH.2025.0007

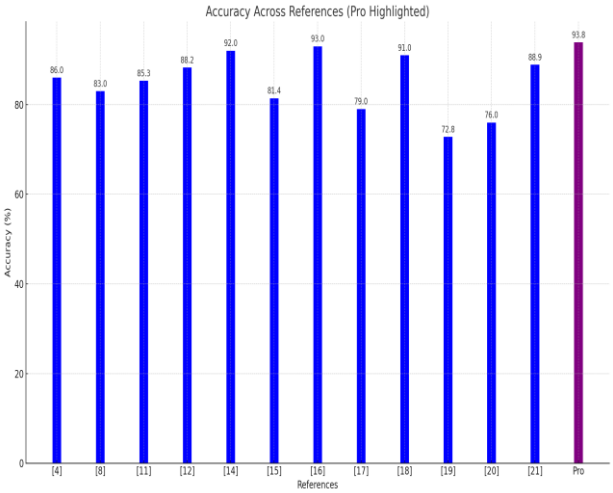

Figure 8 Accuracy

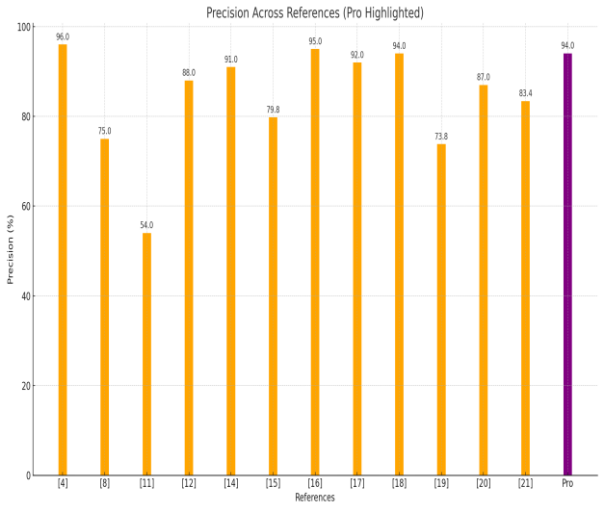

Figure 9 Precision

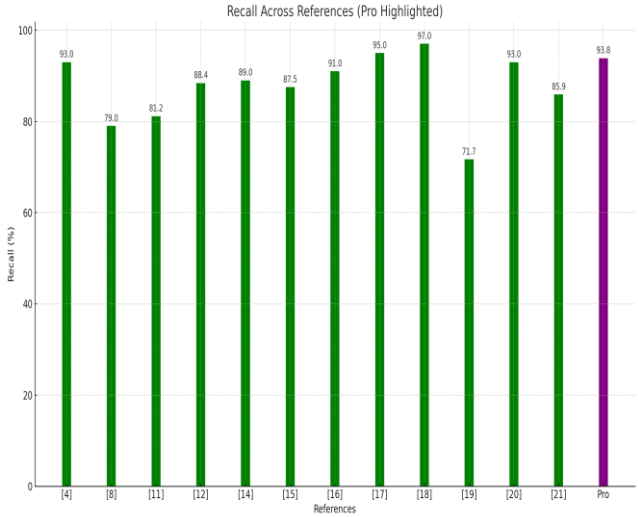

Figure 10 Recall

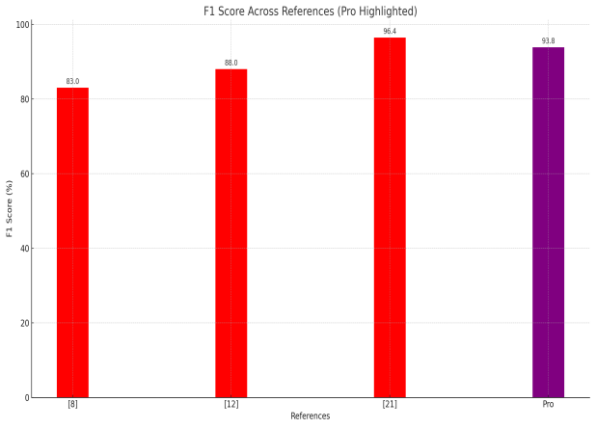

Figure 11 F1 Score

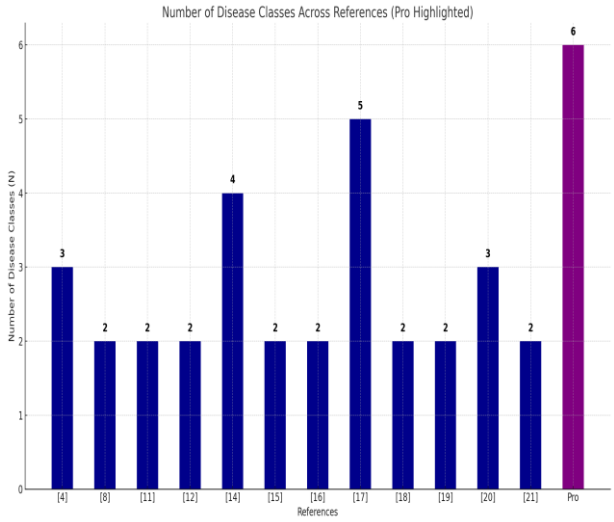

Figure 12 Diseases classifying capability

The proposed model exhibits outstanding performance when compared to other references. It handles six disease classes, which is more than any other reference. The model has an accuracy of 93.85%, outperforming other references. Also, precision of 94.04%, recall of 93.85%, and F1 score of 93.82% showcase its balanced performance, classifying six disease classes. Figure 8 shows Accuracy, Figure 9 shows Precision, Figure 10 shows Recall, Figure 11 shows F1 Score, Figure 12 shows Diseases classifying capability.

Conclusion and Future Scope

The transfer learning-based CNN model was developed for the six-class lung disease classification (pneumonia, cardiomegaly, lung opacity, TB, COVID-19, and normal) using CXR images. The transfer learning was performed with extended-

International Research Journal on Advanced Engineering Hub (IRJAEH)
e ISSN: 2584-2137
Vol. 03 Issue: 01 January 2025
Page No: 52-60
https://irjaeh.com
https://doi.org/10.47392/IRJAEH.2025.0007

VGG19 architecture. The model was refined using hyperparameters such as l_r, e_n, and b_s with 10^{-5}, 50, and 32 respectively. The results confirm that the TL-CNN exhibits superior performance when compared to existing models. The accuracy, precision, sensitivity, F1 score, and AUC of the TL-CNN were found to be 93.85%, 94.04%, 93.85%, 93.82% and 99.56%, respectively. Additionally, the distinguishability of the proposed six-class lung disease classification model is confirmed using TL-CNN confusion matrix. The Python code of the developed model was published on the publicly available websites Kaggle [28] and GitHub [29].Future research could explore the combination of modalities such as CXR, CT images, and sound files to further enhance the performance. Collaboration with healthcare providers for clinical validation can be conducted to deploy the model as a practical tool.

References

[1] Thirumaladevi, S., Veera Swamy, K., & Sailaja, M. (2022). Improved transfer learning of CNN through fine-tuning and classifier ensemble for scene classification. Soft Computing, 26, 5617–5636. https://doi.org/10.1007/s00500-022-07145

[2] Sairam, M. V. S., Egala, R., Rajasekhar, H., & Nohith, K. S. (2024). Deep Learning-Based Spectrum Management to Enhance the Performance of Cognitive Radio Network Using MobileNet. IRE Journals, 8(6), 274-279.

[3] Egala, R., Sairam, M. V. S., & Anusha, J. (2025). Improving Cognitive Radio Network Performance Using AlexNet. International Journal of Current Science (IJCSPUB), 15(1), 174-181.

[4] Song, Y., et al. (2021). Deep learning Enables Accurate Diagnosis of Novel Coronavirus (COVID-19) with CT images. IEEE/ACM Transactions on Computational Biology and Bioinformatics, 18(6), 2775-2780. doi: 10.1109/TCBB.2021.3065361

[5] Bai, H.X., et al. (2020). Performance of Radiologists in Differentiating COVID-19 from Non-COVID-19 Viral Pneumonia at Chest CT. Radiology, 296(2), E46-E54. https://doi.org/10.1148/radiol.2020200823

[6] Sairam, M.V.S., Egala, R., & Nohith, K.S. (2024). Deep Learning Framework for Enhancing the Performance of Cognitive Radio Network. Journal of Emerging Technologies and Innovative Research, 11(11). http://doi.one/10.1729/Journal.42133

[7] Egala, R., & Sairam, M. V. S. (2024). A Review on Medical Image Analysis Using Deep Learning. Engineering Proceeding, 66(1), 7. https:// doi.org/ 10.3390/engproc2024066007

[8] Sirazitdinov, I., et al. (2019). Deep neural network ensemble for pneumonia localization from a large-scale chest x-ray database. Computers and Electrical Engineering, 78, 388-399. https:// doi.org/ 10.1016/ j.compeleceng.2019.08.004

[9] Pavani, P. G., Biswal, B., Sairam, M. V. S. S., & Subrahmanyam, N. B. (2021). A semantic contour-based segmentation of lungs from chest x-rays for the classification of tuberculosis using Naïve Bayes classifier. International Journal of Imaging Systems and Technology, 31(4), 870-881. https:// doi.org/ 10.1002/ima.22556

[10] Gao, X.W., James-Reynolds, C., & Currie, E. (2020). Analysis of tuberculosis severity levels from CT pulmonary images-based on enhanced residual deep learning architecture. Neurocomputing, 392, 233-344. http:// dx.doi.org/10.1016/j.neucom.2018.12.086

[11] Hooda, R., et al. (2019). Automated TB classification using ensemble of deep architectures. Multimedia Tools and Applications, 78(22), 31515-31532. https:// link.springer.com/article/ 10.1007/s11042-019-07984-5

[12] Zak, M., & Krzyżak, J. (2020). Classification of Lung Diseases Using Deep Learning Models. In Computational Science (pp. 621-634). https:// doi.org/ 10.1007/978-3-030-50420-5_47

[13] Chalie, M., & Mossie, Z. (2023). Pulmonary disease identification and classification using deep learning approach. European International Journal of Science and

Technology, 1(2), 39-49. https://doi.org/10.59122/144CFC16

[14] Li, C., et al. (2020). Classification of Severe and Critical Covid-19 Using Deep Learning and Radiomics. IEEE Journal of Biomedical and Health Informatics, 24(12), 3585-3594. doi: 10.1109/jbhi.2020.3036722

[15] Pathak, Y., et al. (2020). Deep Transfer Learning Based Classification Model for COVID-19 Disease. Biomedical Research and Engineering, 43(2), 87-92. doi: 10.1016/j.irbm.2020.05.003

[16] Sitaula, C., & Hossain, M.B. (2020). Attention-based VGG-16 model for COVID-19 chest X-ray image classification. Applied Intelligence, 51(5), 2850-2863. https://doi.org/10.1007/s10489-020-02055-x

[17] Dansana, D., et al. (2020). Early diagnosis of COVID-19-affected patients-based on X-ray and computed tomography images using deep learning algorithm. Soft Computing, 27(5), 2635-2643. https://doi.org/10.1007/s00500-020-05275-y

[18] Zhang, J., et al. (2020). COVID-19 screening on chest X-ray images using deep learning-based anomaly detection. arXiv. Retrieved fromhttps://www.researchgate.net/publication/340271344_COVID19_Screening_on_Chest_Xray_Images_Using_Deep_Learning_based_Anomaly_Detection

[19] Tsiknakis, N., et al. (2020). Interpretable artificial intelligence framework for COVID-19 screening on chest X-rays. Experimental and Therapeutic Medicine, 20(2), 727-735. https:/ /doi.org/ 10.3892/ etm.2020.8797

[20] Oh, Y., Park, S., & Ye, J.C. (2020). Deep Learning COVID-19 Features on CXR Using Limited Training Data Sets. IEEE Transactions on Medical Imaging, 39(8), 2688-2700. doi: 10.1109/TMI.2020.2993291

[21] Hassantabar, S., et al. (2020). Diagnosis and detection of infected tissue of COVID-19 patients based on lung x-ray image using convolutional neural network approaches. Chaos, Solitons & Fractals, 140, 960-0779. https://doi.org/10.1016/j.chaos.2020.110170

[22] Fawad, et al. (2022). Chest X-ray Classification for the Detection of COVID-19 Using Deep Learning Techniques. Sensors, 22(3), 1211. https:// doi.org/ 10.3390/ s22031211

[23] Putri, K.A., & Al Maki, W.F. (2023). Enhancing Pneumonia Disease Classification using Genetic Algorithm-Tuned DCGANs and VGG-16 Integration. Jurusan Teknik Elektromedik (JEEEMI), 6(1). https:// doi.org/10.35882/jeeemi.v6i1.349

[24] Kingma, D.P., & Ba, J. (2014). Adam: A Method for Stochastic Optimization. arXiv:1412.6980. Gulli, A., & Pal, S. (2017). Deep Learning with Keras. Packt Publishing Ltd. Mooney, P.T. (n.d.). Chest X-ray pneumonia dataset. Kaggle.

[25] Khan, M.A., & Algarni, F. (2020). A Healthcare Monitoring System for the Diagnosis of Heart Disease in the IoMT Cloud Environment Using MSSO-ANFIS. IEEE Access, 8, 122259-122269. https://doi.org/10.1109/ACCESS.2020.3006424

[26] https://github.com/RAJUEGALA/TRANSFERLEARNING/blob/main/Transfer%20Learning.ipynb